AFRL-AFOSR-VA-TR-2019-0095

Efficient and Robust High-Order Methods for Fluid and Solid Mechanics

Per-Olof Persson
REGENTS OF THE UNIVERSITY OF CALIFORNIA

02/01/2019
Final Report

Air Force Research Laboratory
AF Office Of Scientific Research (AFOSR)/ RTA2
Arlington, Virginia 22203
Air Force Materiel Command

DISTRIBUTION A: Distribution approved for public release.

REPORT DOCUMENTATION PAGE

Form Approved
OMB No. 0704–0188

1. REPORT DATE *(DD–MM–YYYY)*	2. REPORT TYPE	3. DATES COVERED *(From — To)*
01–31–2019	Final	1 Nov 2014 — 31 Oct 2018

4. TITLE AND SUBTITLE

EFFICIENT AND ROBUST HIGH-ORDER METHODS FOR FLUID AND SOLID MECHANICS

5a. CONTRACT NUMBER

5b. GRANT NUMBER

FA9550-15-1-0010

5c. PROGRAM ELEMENT NUMBER

6. AUTHOR(S)

Persson, Per-Olof

5d. PROJECT NUMBER

5e. TASK NUMBER

5f. WORK UNIT NUMBER

7. PERFORMING ORGANIZATION NAME(S) AND ADDRESS(ES)

Department of Mathematics
University of California, Berkeley
Berkeley, CA 94720–3840

8. PERFORMING ORGANIZATION REPORT NUMBER

9. SPONSORING / MONITORING AGENCY NAME(S) AND ADDRESS(ES)

AFOSR/RSL
875 North Randolph Street
Suite 325, Room 3112
Arlington, VA 22203

10. SPONSOR/MONITOR'S ACRONYM(S)

AFOSR

11. SPONSOR/MONITOR'S REPORT NUMBER(S)

12. DISTRIBUTION / AVAILABILITY STATEMENT

Approval for public release; distribution is unlimited.

13. SUPPLEMENTARY NOTES

14. ABSTRACT

The goal of the project was to develop new numerical schemes and solvers for high-order accurate simulations of problems in fluid and solid mechanics. Three main areas were addressed – space-time methods for domains with large deformations, implicit matrix-free solvers for sparse line-based discretizations, and applications to problems with highly turbulent flow. The project has led to significant developments in space-time mesh generation for complex flow problems, entropy stable line-based discontinuous Galerkin discretizations, low-memory Kronecker SVD factorizations applied to preconditioning, practical solvers for fully implicit Runge-Kutta methods, partitioned multiphysics solvers based on IMEX schemes, and new high-order schemes for shock tracking. The results were applied to important real-world problems, such as the high-order simulation of shock boundary-layer interaction. The findings were disseminated through a wide range of publications, presentations, and public domain software.

15. SUBJECT TERMS

16. SECURITY CLASSIFICATION OF:			17. LIMITATION OF ABSTRACT	18. NUMBER OF PAGES	19a. NAME OF RESPONSIBLE PERSON
a. REPORT	b. ABSTRACT	c. THIS PAGE			Dr. Per-Olof Persson
U	U	U	UU	22	19b. TELEPHONE NUMBER *(include area code)* (510) 642–6947

FINAL REPORT

EFFICIENT AND ROBUST HIGH-ORDER METHODS FOR FLUID AND SOLID MECHANICS

Per-Olof Persson

Department of Mathematics
University of California, Berkeley
Berkeley, CA 94720–3840

January 2019

Grant number: FA9550-15-1-0010

Dates covered: 1 Nov 2014 — 31 Oct 2018

Abstract

The goal of the project was to develop new numerical schemes and solvers for high-order accurate simulations of problems in fluid and solid mechanics. Three main areas were addressed – space-time methods for domains with large deformations, implicit matrix-free solvers for sparse line-based discretizations, and applications to problems with highly turbulent flow. The project has led to significant developments in space-time mesh generation for complex flow problems, entropy stable line-based discontinuous Galerkin discretizations, low-memory Kronecker SVD factorizations applied to preconditioning, practical solvers for fully implicit Runge-Kutta methods, partitioned multiphysics solvers based on IMEX schemes, and new high-order schemes for shock tracking. The results were applied to important real-world problems, such as the high-order simulation of shock boundary-layer interaction. The findings were disseminated through a wide range of publications, presentations, and public domain software.

REPORT DOCUMENTATION PAGE

Form Approved
OMB No. 0704–0188

1. REPORT DATE *(DD–MM–YYYY)*	2. REPORT TYPE	3. DATES COVERED *(From — To)*
01–31–2019	Final	1 Nov 2014 — 31 Oct 2018

4. TITLE AND SUBTITLE

EFFICIENT AND ROBUST HIGH-ORDER METHODS FOR FLUID AND SOLID MECHANICS

5a. CONTRACT NUMBER

5b. GRANT NUMBER

FA9550-15-1-0010

5c. PROGRAM ELEMENT NUMBER

6. AUTHOR(S)

Persson, Per-Olof

5d. PROJECT NUMBER

5e. TASK NUMBER

5f. WORK UNIT NUMBER

7. PERFORMING ORGANIZATION NAME(S) AND ADDRESS(ES)

Department of Mathematics
University of California, Berkeley
Berkeley, CA 94720–3840

8. PERFORMING ORGANIZATION REPORT NUMBER

9. SPONSORING / MONITORING AGENCY NAME(S) AND ADDRESS(ES)

AFOSR/RSL
875 North Randolph Street
Suite 325, Room 3112
Arlington, VA 22203

10. SPONSOR/MONITOR'S ACRONYM(S)

AFOSR

11. SPONSOR/MONITOR'S REPORT NUMBER(S)

12. DISTRIBUTION / AVAILABILITY STATEMENT

Approval for public release; distribution is unlimited.

13. SUPPLEMENTARY NOTES

14. ABSTRACT

The goal of the project was to develop new numerical schemes and solvers for high-order accurate simulations of problems in fluid and solid mechanics. Three main areas were addressed – space-time methods for domains with large deformations, implicit matrix-free solvers for sparse line-based discretizations, and applications to problems with highly turbulent flow. The project has led to significant developments in space-time mesh generation for complex flow problems, entropy stable line-based discontinuous Galerkin discretizations, low-memory Kronecker SVD factorizations applied to preconditioning, practical solvers for fully implicit Runge-Kutta methods, partitioned multiphysics solvers based on IMEX schemes, and new high-order schemes for shock tracking. The results were applied to important real-world problems, such as the high-order simulation of shock boundary-layer interaction. The findings were disseminated through a wide range of publications, presentations, and public domain software.

15. SUBJECT TERMS

16. SECURITY CLASSIFICATION OF:			17. LIMITATION OF ABSTRACT	18. NUMBER OF PAGES	19a. NAME OF RESPONSIBLE PERSON
a. REPORT	b. ABSTRACT	c. THIS PAGE			Dr. Per-Olof Persson
U	U	U	UU	22	19b. TELEPHONE NUMBER *(include area code)* (510) 642–6947

Efficient and Robust High-Order Methods for Fluid and Solid Mechanics

P.-O. Persson, Dept. of Mathematics, University of California, Berkeley

Objectives

The goal of the project was to develop new numerical schemes and solvers for high-order accurate simulations of problems in fluid and solid mechanics. Three main areas were addressed – space-time methods for domains with large deformations, implicit matrix-free solvers for sparse line-based discretizations, and applications to problems with highly turbulent flow. The project has led to significant developments in space-time mesh generation for complex flow problems, entropy stable line-based discontinuous Galerkin discretizations, low-memory Kronecker SVD factorizations applied to preconditioning, practical solvers for fully implicit Runge-Kutta methods, partitioned multiphysics solvers based on IMEX schemes, and new high-order schemes for shock tracking. The results were applied to important real-world problems, such as the high-order simulation of shock boundary-layer interaction. The findings were disseminated through a wide range of publications, presentations, and public domain software.

Accomplishments

During the award period, we have conducted several significant research efforts in the general area of high-order accurate numerical methods for solving partial differential equations on unstructured meshes. It is widely believed that these new methods will eventually replace the more traditional simulation techniques for challenging problems in fluid and solid mechanics, for example with propagating waves, turbulent flow, nonlinear interactions, and multiple scales. However, several new developments are required to make high-order methods competitive, such as more efficient numerical solvers and increased robustness. Our work has addressed many of these issues, and below we summarize the research that we have carried out.

High-Order Space-Time Discontinuous Galerkin Methods for Moving Domains

Here, we give a concise summary of our work on space-time meshes and discontinuous Galerkin methods. For more details, see [2, 4, 3].

Motivation

A challenging problem in the numerical solution of PDEs is how to obtain high-order accuracy in the presence of moving domains with large deformations. The popular Arbitrary Lagrangian-Eulerian (ALE) method can be viewed as a mapping-based approach which, together with appropriate treatment of the Geometric Conservation Law (GCL), allows for arbitrarily high orders of accuracy in both space and time. However, the method requires smooth mappings between the initial (or reference) frame and the actual physical configuration. These can be generated for domains undergoing moderate deformations, such as pitching and heaving airfoils, or structures with small deformations. But many other applications require topological changes to maintain a well-shaped mesh/transformation, e.g. rotating machinery or configurations involving multiple moving objects.

In our work [4, 3], we proposed a framework for solving systems of conservation laws on moving meshes to an arbitrary degree of accuracy in both space and time. The method is based on the assumption that the unstructured moving meshes can be produced by a sequence of entirely local operations. This produces high-quality meshes throughout the simulation, and provides a simple description of the mesh changes between each timestep. Using this information we can construct efficient numerical schemes based on high-order discontinuous Galerkin formulations, and we consider both space-time and ALE/projection-based methods in 2D and 3D.

The DistMesh mesh generator

The so-called DistMesh method is based on iterative updates of the positions of the N interior mesh nodes $\boldsymbol{p}^{(n)}$, $n = 1, \ldots, N$, driven by spring-based forces $\boldsymbol{F}_i$ for each edge i adjacent to node n, of the form:

$$\boldsymbol{p}^{(n+1)} = \boldsymbol{p}^{(n)} + \delta \sum_i \boldsymbol{F_i}, \qquad |\boldsymbol{F}_i(l)| = \begin{cases} k(l - l_0) & \text{if } l \geq l_0, \\ 0 & \text{if } l < l_0. \end{cases} \tag{1}$$

Here, δ is a pseudo-timestep, k is the spring constant, l_0 is the desired edge length, and l is the actual edge length. In addition, the mesh generator employs local element topology modifications, such as the simple edge flipping in 2D or more complex operations in 3D. Here, we assume that each element can be flipped once during each sweep, but multiple rounds during each time step.

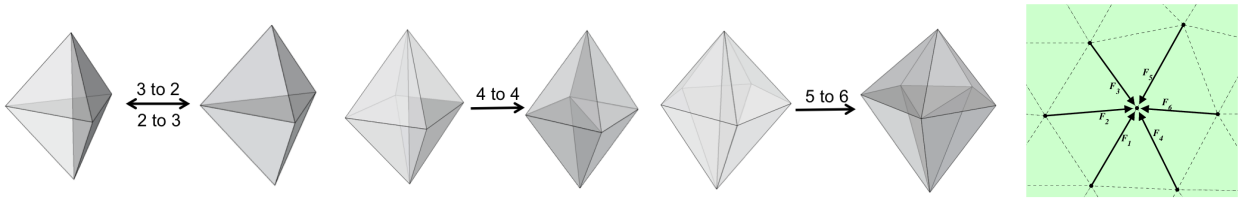

Space-Time mesh generation

Noting that our moving meshes are defined by entirely local operations (node movements and element flips), we are able to define provably good space-time meshes. These are based on fully unstructured simplex elements, that is, tetrahedra in 2D+time and 4D simplices in 3D+time. We restrict our method to slab-based space-time meshing, that is, all elements have uniform size in the temporal direction. However, extending this to adaptivity in time using local refinement should be straight-forward, even for the 4D elements.

The method for choosing appropriate space-time elements is mostly combinatorial, and uses node data only to allow for choosing the highest quality configurations. For details, see [3].

Space-Time discontinuous Galerkin discretization

Using our space-time meshes, we define a high-order accurate discontinuous Galerkin (DG) method as follows. The scheme is based on a fully consistent discretization in both space and time, and allows for arbitrary mesh deformations and topology changes.

Consider a system of conservation laws of the form

$$\frac{\partial \boldsymbol{u}}{\partial t} + \nabla_{\boldsymbol{X}} \cdot \boldsymbol{F}^{\text{inv}}(\boldsymbol{u}) = \nabla_{\boldsymbol{X}} \cdot \boldsymbol{F}^{\text{vis}}(\boldsymbol{u}, \nabla_{\boldsymbol{X}} \boldsymbol{u}) \tag{2}$$

with appropriate initial and boundary conditions. We write this in a space-time form and use the standard technique of splitting into a first-order system:

$$\nabla_{\boldsymbol{XT}} \cdot \tilde{\boldsymbol{F}}^{\text{inv}}(\boldsymbol{u}) = \nabla_{\boldsymbol{X}} \cdot \boldsymbol{F}^{\text{vis}}(\boldsymbol{u}, \boldsymbol{q}), \tag{3}$$

$$\nabla_{\boldsymbol{X}} \boldsymbol{u} = \boldsymbol{q}. \tag{4}$$

Next, we define the broken DG spaces $\mathcal{V}_T^h$ and Σ_T^h associated with a triangulation $\mathcal{T}_{[0,T]}^h = \{K\}$ of the space-time domain $\Omega[0, T]$ as:

$$\mathcal{V}_T^h = \{\boldsymbol{v} \in [L^2(\Omega[0,T])]^5 \mid \boldsymbol{v}|_K \in [\mathcal{P}_p(K)]^5 \ \ \forall K \in \mathcal{T}_{[0,T]}^h\}, \tag{5}$$

$$\Sigma_T^h = \{\boldsymbol{\sigma} \in [L^2(\Omega[0,T])]^{5\times 3} \mid \boldsymbol{\sigma}|_K \in [\mathcal{P}_p(K)]^{5\times 3} \ \ \forall K \in \mathcal{T}_{[0.T]}^h\}, \tag{6}$$

Now, discretize the first-order system using a standard DG formulation on the space-time domain $\Omega[t_1, t_2]$:

$$-\int_K \tilde{\boldsymbol{F}}^{\text{inv}}(\boldsymbol{u}^h) : \nabla_{\boldsymbol{XT}} \boldsymbol{v}^h \, dx + \oint_{\partial K} (\widehat{\tilde{\boldsymbol{F}}^{\text{inv}} \cdot \boldsymbol{n}}) \cdot \boldsymbol{v}^h \, ds$$
$$= -\int_K \boldsymbol{F}^{\text{vis}}(\boldsymbol{u}^h, \boldsymbol{q}^h) : \nabla_{\boldsymbol{X}} \boldsymbol{v}^h \, dx + \oint_{\partial K} (\widehat{\boldsymbol{F}^{\text{vis}} \cdot \boldsymbol{n}_s}) \cdot \boldsymbol{v}^h \, ds, \qquad \forall \boldsymbol{v}^h \in \mathcal{V}_T^h \quad (7)$$

$$\int_K \boldsymbol{q}^h : \boldsymbol{\sigma}^h \, dx = -\int_K \boldsymbol{u}^h \cdot (\nabla_{\boldsymbol{X}} \cdot \boldsymbol{\sigma}^h) \, dx + \oint_{\partial K} (\widehat{\boldsymbol{u}^h} \otimes \boldsymbol{n}_s) : \boldsymbol{\sigma}^h \, ds, \qquad \forall \boldsymbol{\sigma}^h \in \Sigma_T^h. \quad (8)$$

For more details, including the details on how to assemble and solve the resulting nonlinear systems of equations, see [2,3].

Results

To demonstrate the accuracy of our proposed methods, we consider the standard test problem of an isentropic Euler vortex. We use polynomial degrees p of 1, 2, and 3, and obtain numerically the expected optimal orders of accuracy $p+1$. See [2,3] for demonstrations on more complex problems, including flow problems in both 2D and 3D which show the ability of our method to deal with complex domain motions.

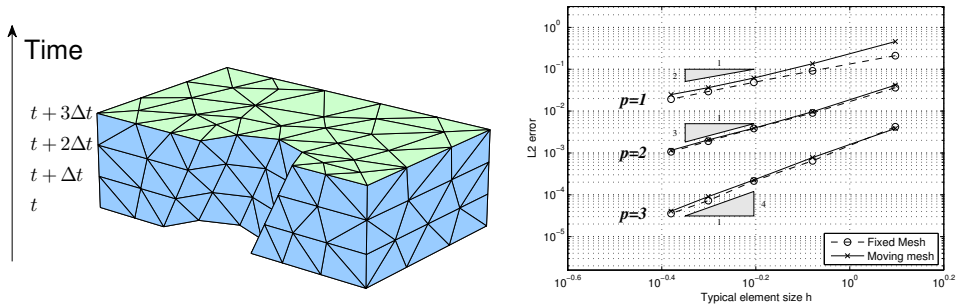

Approximate tensor-product preconditioners for very high order DG methods

Here we provide a short overview of our work on tensor-product preconditioners. More details are provided in [17, 21, 22].

Motivation

The goal of our work is to develop a new tensor-product based preconditioner for discontinuous Galerkin methods with polynomial degrees higher than those typically employed. This preconditioner uses an automatic, purely algebraic method to approximate the exact block Jacobi preconditioner by Kronecker products of several small, one-dimensional matrices. Traditional matrix-based preconditioners require $\mathcal{O}(p^{2d})$ storage and $\mathcal{O}(p^{3d})$ computational work, where p is the degree of basis polynomials used, and d is the spatial dimension. Our SVD-based tensor-product preconditioner requires $\mathcal{O}(p^{d+1})$ storage, $\mathcal{O}(p^{d+1})$ work in two spatial dimensions, and $\mathcal{O}(p^{d+2})$ work in three spatial dimensions. Combined with a matrix-free Newton-Krylov solver, these preconditioners allow for the solution of DG systems in linear time in p per degree of freedom in 2D, and reduce the computational complexity from $\mathcal{O}(p^9)$ to $\mathcal{O}(p^5)$ in 3D. Numerical results are shown in 2D and 3D for the advection, Euler, and Navier-Stokes equations, using polynomials of degree up to $p = 30$. For many test cases, the preconditioner results in similar iteration counts when compared with the exact block Jacobi preconditioner, and performance is significantly improved for high polynomial degrees p.

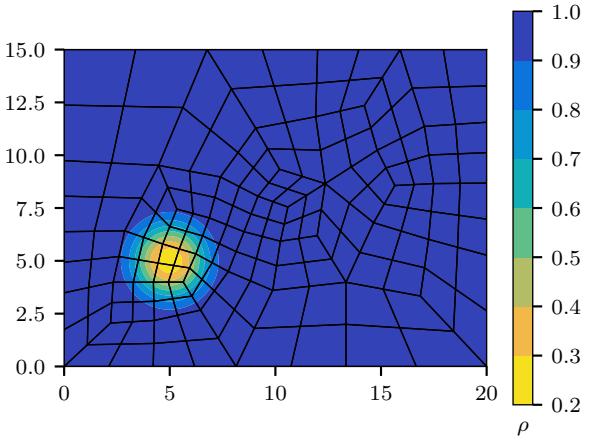

Figure 1: Initial conditions (density) for Euler vortex on unstructured mesh.

Tensor-product preconditioners

We draw inspiration from the tensor-product structure often seen in finite-difference and spectral approximations to, *e.g.* the Laplacian operator on a n^d cartesian grid, which can be written in one, two, and three spatial dimensions, respectively, as

$$L_{1\mathrm{D}} = T_n, \qquad L_{2\mathrm{D}} = I \otimes T_n + T_n \otimes I, \qquad L_{3\mathrm{D}} = I \otimes I \otimes T_n + I \otimes T_n \otimes I + T_n \otimes I \otimes I, \tag{9}$$

where T_n is the standard one-dimensional approximation to the Laplacian. Given a general conservation law, the flux function F is not required to possess any particular structure, and thus the DG discretization of such a function will not be exactly expressible in a similar tensor-product form. That being said, many of the key operations in DG are expressible in a similar form. Therefore, in order to precondition a diagonal block A of a matrix, we look for tensor-product approximations of the form

$$A \approx P = \sum_{j=1}^{r} A_j \otimes B_j \qquad \text{in 2D}, \tag{10}$$

$$A \approx P = \sum_{j=1}^{r} A_j \otimes B_j \otimes C_j \qquad \text{in 3D}, \tag{11}$$

for a fixed number of terms r, where each of the matrices A_j, B_j, and C_j are of size $(p+1)\times(p+1)$. Given r, it is possible to find the best possible approximation (in the Frobenius norm) of the form (10) to an arbitrary given matrix by means of the Kronecker-product singular value decomposition (KSVD).

Results

As an example, we consider the compressible Euler equations of gas dynamics in two dimensions. A typical model problem of an Euler vortex is shown in Figure 1. In our performance evaluation, we compare the runtime of the Kronecker-product preconditioner with the exact block Jacobi preconditioner. Although we have observed that for large time steps Δt or polynomial degrees p, the KSVD preconditioner requires more iterations to converge, it is also possible to compute and apply this preconditioner much more efficiently. Here, we compare the wall-clock time required

to compute and apply the preconditioner, respectively, for $p = 3, 4, \ldots, 15$. The block Jacobi preconditioner is computed by first assembling the diagonal block of the Jacobian matrix using an efficient sum-factorized form, and then computing its LU factorization. The wall-clock times for these operations are shown in Figure 2. We remark that we observe the expected asymptotic computational complexities for each of these operations, where forming the Jacobi preconditioner requires $\mathcal{O}(p^6)$ operations, and applying the Jacobi preconditioner requires $\mathcal{O}(p^4)$ operations. Both forming and applying the approximate Kronecker-product preconditioner can be done in $\mathcal{O}(p^3)$ time.

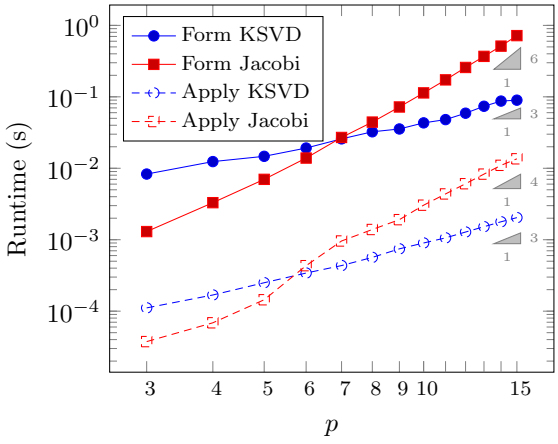

Figure 2: Wall-clock time required to form and apply the KSVD and Jacobi preconditioners

Future work for further improving the performance of this preconditioner include systematic treatment of viscous fluxes and second-order terms, and fast inversion of sums of more than two Kronecker products allowing for treatment of off-diagonal blocks in the context of an ILU-based preconditioner. Also of interest is the investigation of the performance of the preconditioner when used as a smoother in p-multigrid solvers.

Stage-Parallel Implicit Runge-Kutta Time-Integration

Here, we give a concise summary of our recent work on fully Implicit Parallel-in-Time Runge-Kutta solvers. The details are reported in our JCP paper [16].

Motivation

Implicit time integration methods for DG have been much studied. Both the multi-step backward differentiation formulas (BDF) and single-step diagonally implicit Runge-Kutta (DIRK) methods have been successfully applied to discontinuous Galerkin discretizations for fluid flow problems. These methods have some limitations: BDF schemes can be A-stable only up to second-order (the famous second Dahlquist barrier), a severe limitation when used in conjunction with a high-order spatial discretization. On the other hand, there exist high-order A-stable (and even L-stable) DIRK schemes, but these methods have a low stage-order, often resulting in order reduction when applied to stiff problems.

The Radau IIA methods, one class of the so-called fully implicit Runge-Kutta (IRK) methods, are high-order, L-stable, and have relatively high stage order. These methods suffer less from order reduction when applied to stiff problems, and they require only a small number of stages s, with the order of accuracy given by $p = 2s - 1$. They have the drawback that each step involves the

solution of large, coupled linear systems of equations. The difficulty in efficiently implementing such methods has caused them to remain not widely used or studied for practical applications.

In our work, we have developed a new strategy for efficiently solving the resulting large linear systems by means of the iterative preconditioned GMRES algorithm. A simple transformation of the linear system results in a significant reduction of the cost per GMRES iteration. Furthermore, the block ILU(0) preconditioner, used successfully with implicit time-integrators for the discontinuous Galerkin method before, proves to be effective also for these large systems. A shifted, uncoupled, block ILU(0) factorization is also found to be an effective preconditioner, with the advantage of allowing parallelism in time by computing the stage solutions simultaneously.

Implicit Runge-Kutta Methods

A general s-stage Implicit Runge-Kutta (IRK) Method for the system of ODEs $\boldsymbol{M}\frac{\partial \boldsymbol{u}}{\partial t} = \boldsymbol{f}(\boldsymbol{u})$ has the form

$$\boldsymbol{M}\boldsymbol{k}_i = \boldsymbol{f}\left(t_0 + \Delta t c_i, \boldsymbol{u}_0 + \Delta t \sum_{j=1}^{s} a_{ij}\boldsymbol{k}_j\right), \tag{12}$$

$$\boldsymbol{u}_1 = \boldsymbol{u}_0 + \Delta t \sum_{i=1}^{s} b_i \boldsymbol{k}_i. \tag{13}$$

The coefficients can be expressed compactly in the form of the *Butcher tableau*,

$$\begin{array}{c|ccc} c_1 & a_{11} & \cdots & a_{1s} \\ \vdots & \vdots & \ddots & \vdots \\ c_s & a_{s1} & \cdots & a_{ss} \\ \hline & b_1 & \cdots & b_s \end{array} = \begin{array}{c|c} \boldsymbol{c} & A \\ \hline & \boldsymbol{b}^T \end{array}. \tag{14}$$

A number of well-known properties can be determined directly from this form: (i) for a general Butcher tableau A, the method is called an Implicit Runge-Kutta method (IRK), (ii) for A lower triangular, the method decouples into s separate implicit systems and is called a Diagonally IRK method (DIRK), (iii), if the method is A-stable, A is invertible, and $a_{s,i} = b_i$, then the method is also L-stable. Here, we only consider L-stable schemes since this appears to be a requirement for real-world CFD computations. We study a number of DIRK and Radau IIA schemes.

Efficient solution of IRK systems

For increased sparsity in the corresponding nonlinear systems, we change variables from stage derivatives $\boldsymbol{K}$

$$\left(I_s \otimes \boldsymbol{M} - \Delta t \begin{pmatrix} a_{11}\boldsymbol{J}_1 & \cdots & a_{1s}\boldsymbol{J}_1 \\ \vdots & \ddots & \vdots \\ a_{s1}\boldsymbol{J}_s & \cdots & a_{ss}\boldsymbol{J}_s \end{pmatrix}\right)\boldsymbol{K} = \boldsymbol{R}, \tag{15}$$

into stage solutions $\boldsymbol{W} = (A \otimes I_n)\boldsymbol{K}$:

$$\left(A^{-1} \otimes \boldsymbol{M} - \Delta t \begin{pmatrix} \boldsymbol{J}_1 & 0 & \cdots & 0 \\ 0 & \boldsymbol{J}_2 & \cdots & 0 \\ \vdots & \vdots & \ddots & \vdots \\ 0 & 0 & \cdots & \boldsymbol{J}_s \end{pmatrix}\right)\boldsymbol{W} = \boldsymbol{R}. \tag{16}$$

Figure 3: Stage-parallel partitioning of the matrix $\boldsymbol{B} = \boldsymbol{A}^{-1} \otimes \boldsymbol{M} - \Delta t \begin{pmatrix} \boldsymbol{J}_1 & 0 \\ 0 & \boldsymbol{J}_2 \end{pmatrix}$. The color of the matrix entries indicates the node to which it belongs.

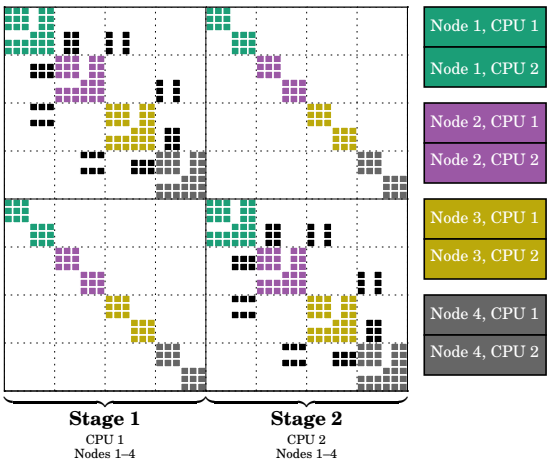

This reduces the cost of matrix-vector multiplication, to scale almost linearly with s. Next we introduce a stage-uncoupled shifted block ILU(0), which ignores the coupling between stages in the preconditioner:

$$\begin{pmatrix} \tilde{\boldsymbol{L}}_1\tilde{\boldsymbol{U}}_1 & 0 & \cdots & 0 \\ 0 & \tilde{\boldsymbol{L}}_2\tilde{\boldsymbol{U}}_2 & \cdots & 0 \\ \vdots & \vdots & \ddots & \vdots \\ 0 & 0 & \cdots & \tilde{\boldsymbol{L}}_s\tilde{\boldsymbol{U}}_s \end{pmatrix}, \tag{17}$$

where $\tilde{\boldsymbol{L}}_i\tilde{\boldsymbol{U}}_i$ is the block ILU(0) factorization of a matrix of the form $\left(A_{ii}^{-1} + \alpha_i\right)\boldsymbol{M} - \Delta t \boldsymbol{J}_i$. The *shifts* α_i compensate for the ignored mass matrices, an emperically good choice is $\alpha_i = \sum_{j \neq i} \left| A_{ji}^{-1} \right|$.

This stage-uncoupled preconditioner is not only efficient in serial, but also allows for perfect parallelization *across* the stages. The high level of communication between the stages can be resolved by scheduling to shared memory compute nodes, which is illustrated in Figure 3. This effectively results in a factor of s smaller domain decompositions, with better ILU performance and better strong scaling.

Results

For examples of the performance of the methods, we study the LES flow around a NACA airfoil at high angle-of-attack and Reynolds number 40,000. Figure 4 (left) shows the error vs. computational work for two high-order IRK and DIRK methods, which shows that in general the IRK schemes outperform the traditional DIRK schemes significantly.

To demonstrate the parallel performance, we solve a large-scale similar 3D problem. Figure 4 (right) shows the number of matrix-vector multiplications as a function of number of compute processes, which is generally an increasing dependency because of the parallelization of the ILU preconditioner. However, the stage-parallel solver (P) reduces this effect. In addition, although not measured in these plots, the stage-parallelism should also increase the strong scaling by roughly a factor of s.

IMEX-based partitioned time-integration of multiphysics problems

Here, we give a short summary of our recent work on IMEX-based partitioned time-integration for general multiphysics problems. For more details, see [23, 31, 27].

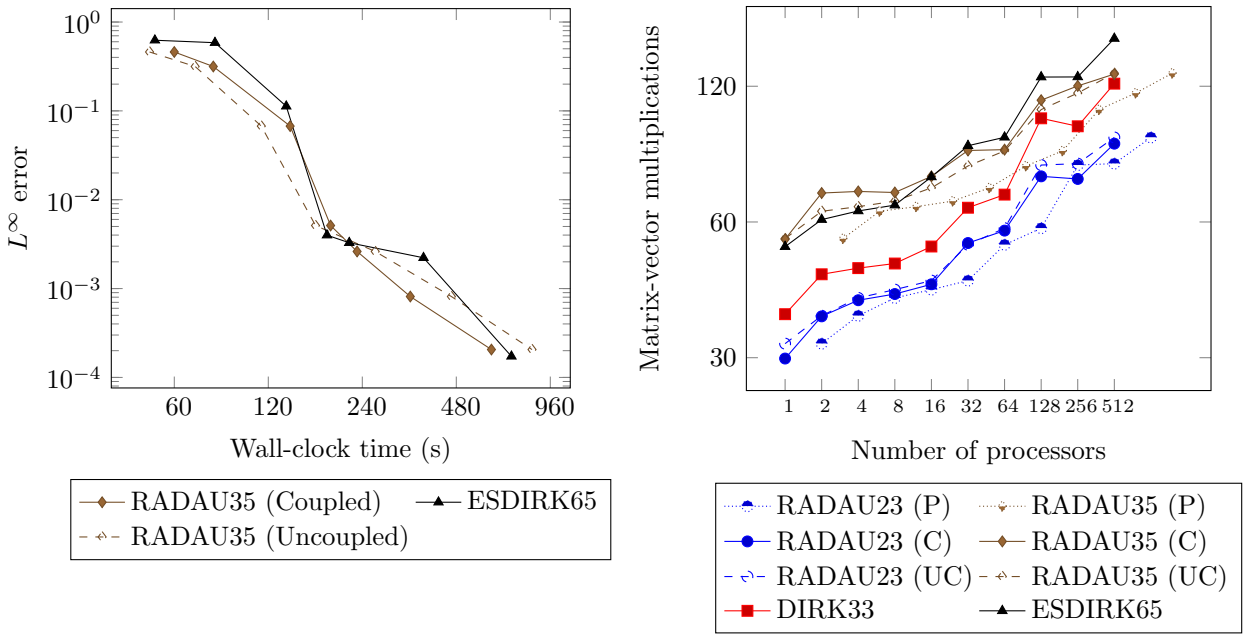

Figure 4: Log-log plots of L^∞ errors vs. wall-clock time for the NACA LES test case (left). Log-log plot of average number of equivalent multiplications vs. number of processes (right).

Motivation

We have previously proposed a high-order accurate time-integrator for coupled Fluid-Structure Interaction (FSI) problems, based on Runge-Kutta IMEX schemes [1]. In our current work, we are extending this method to more general multiphysics problems, and in particular to the so-called 2-field and 3-field formulations for FSI problems. The result is an efficient time-integrator that de-couples the solution process for each physical regime, while retaining the high-order temporal accuracy.

Overview of n-way coupled multiphysics setting

We have completed the implementation of a general n-way coupled multiphysics environment that is being used in a 2-field and 3-field fluid-structure interaction setting. The multiphysics environment is based on n single-physics discretizations, each of which depends on its own state as well as a coupling term. Let $\boldsymbol{r}_i$ denote the spatial discretization of the ith single physics equation, $\boldsymbol{u}_i$ and $\boldsymbol{c}_i$ denote the corresponding state and coupling term, $\boldsymbol{M}_i$ is the mass matrix, and $\boldsymbol{\mu}$ a vector of parameters

$$\boldsymbol{M}_i \dot{\boldsymbol{u}}_i = \boldsymbol{r}_i(\boldsymbol{u}_i, \boldsymbol{c}_i, \boldsymbol{\mu}), \qquad i = 1, \ldots, n.$$

In general, the coupling term $\boldsymbol{c}_i$ will depend on all of the state $\boldsymbol{u}_1, \ldots, \boldsymbol{u}_n$, therefore coupling all equations

$$\boldsymbol{M}_i \dot{\boldsymbol{u}}_i = \boldsymbol{r}_i(\boldsymbol{u}_i, \boldsymbol{c}_i(\boldsymbol{u}_1, \ldots, \boldsymbol{u}_n, \boldsymbol{\mu}), \boldsymbol{\mu}) = 0, \qquad i = 1, \ldots, n.$$

In the 2-field FSI setting, the fluid, based on a Arbitrary Lagrangian-Eulerian (ALE) formulation, is taken as the first single physics equation and we are currently considering a simple model problem for the structure that consists of a mass-spring-damper system

$$\boldsymbol{M}_f \dot{\boldsymbol{u}}_f = \boldsymbol{r}_f(\boldsymbol{u}_f, \boldsymbol{c}_f, \boldsymbol{\mu})$$
$$\boldsymbol{M}_s \dot{\boldsymbol{u}}_s = \boldsymbol{r}_s(\boldsymbol{u}_s, \boldsymbol{c}_s, \boldsymbol{\mu}).$$

The fluid state, $\boldsymbol{u}_f$, is the ALE-transformed fluid state and the coupling term, $\boldsymbol{c}_f$, consists of the fluid mesh position, $\boldsymbol{x}$, and velocity, $\dot{\boldsymbol{x}}$. The structure coupling term, $\boldsymbol{c}_s$, is the force applied to the mass in the mass-spring-damper system. The individual physics are coupled as follows: the fluid mesh position/velocity depends on the structure state and the force on the structure depends on the structure's position as well as the fluid state

$$\begin{aligned}\boldsymbol{c}_f(\boldsymbol{u}_f,\, \boldsymbol{u}_s) &= (\boldsymbol{x}(\boldsymbol{u}_s),\, \dot{\boldsymbol{x}}(\boldsymbol{u}_s)) \\ \boldsymbol{c}_s(\boldsymbol{u}_f,\, \boldsymbol{u}_s) &= \boldsymbol{t}(\boldsymbol{u}_f,\, \boldsymbol{u}_s).\end{aligned}$$

We have also implemented a 3-field FSI approach where the fluid, structure, and mesh deformation are taken as separate fields.

This framework has been implemented in a modular and extensible C++ environment and currently uses 3DG for the fluid solver and in-house structure and mesh motion solvers.

IMEX Runge-Kutta solver for high-order partitioned temporal integration

With the general form of the n-way multiphysics coupling established, we turned to a high-order *partitioned* temporal solver, that is, allows the re-use of single-physics solvers while achieving high-order accuracy and maintaining stability. For this purpose, we use an additive Implicit-Explicit Runge-Kutta (IMEX-RK) solver with carefully chosen implicit/explicit partition that ensures single-physics solvers can be re-used. To demonstrate the solver, the special case of 2-field FSI is considered

$$\begin{aligned}\boldsymbol{M}_f \dot{\boldsymbol{u}}_f &= \boldsymbol{r}_f(\boldsymbol{u}_f,\, \boldsymbol{c}_f(\boldsymbol{u}_f,\, \boldsymbol{u}_s),\, \boldsymbol{\mu}) \\ \boldsymbol{M}_s \dot{\boldsymbol{u}}_s &= \boldsymbol{r}_s(\boldsymbol{u}_s,\, \boldsymbol{c}_s(\boldsymbol{u}_f,\, \boldsymbol{u}_s),\, \boldsymbol{\mu}).\end{aligned}$$

This can be abstracted into the following monolithic system

$$\boldsymbol{M}\boldsymbol{u} = \boldsymbol{f}(\boldsymbol{u},\, \boldsymbol{\mu}) + \boldsymbol{g}(\boldsymbol{u},\, \boldsymbol{\mu})$$

where the mass matrix and state vector are

$$\boldsymbol{M} = \begin{bmatrix}\boldsymbol{M}_f & \\ & \boldsymbol{M}_s\end{bmatrix}, \qquad \boldsymbol{u} = \begin{bmatrix}\boldsymbol{u}_f \\ \boldsymbol{u}_s\end{bmatrix}$$

and the right-hand-side has been additively split into two terms: one which will be handled implicitly ($\boldsymbol{g}$) and one explicitly ($\boldsymbol{f}$). Let $\tilde{\boldsymbol{c}}_s$ be a prediction of $\boldsymbol{c}_s(\boldsymbol{u}_f,\, \boldsymbol{u}_s)$ that depends solely on the solution at *previous timesteps*. Then the following choice for the additive decomposition leads to a partitioned method since the structure component of the implicit term is independent of the fluid

$$\boldsymbol{f} = \begin{bmatrix}\\ \boldsymbol{r}_s(\boldsymbol{u}_s,\, \boldsymbol{c}_s(\boldsymbol{u}_f,\, \boldsymbol{u}_s),\, \boldsymbol{\mu}) - \boldsymbol{r}_s(\boldsymbol{u}_s,\, \tilde{\boldsymbol{c}}_s,\, \boldsymbol{\mu})\end{bmatrix}, \qquad \boldsymbol{g} = \begin{bmatrix}\boldsymbol{r}_f(\boldsymbol{u}_f,\, \boldsymbol{c}_f(\boldsymbol{u}_f,\, \boldsymbol{u}_s),\, \boldsymbol{\mu}) \\ \boldsymbol{r}_s(\boldsymbol{u}_s,\, \tilde{\boldsymbol{c}}_s,\, \boldsymbol{\mu})\end{bmatrix}.$$

Numerous tests have shown that $\tilde{\boldsymbol{c}}_s = \boldsymbol{c}_s(\boldsymbol{u}_f(t-\Delta t),\, \boldsymbol{u}_s(t-\Delta t))$ works quite well. This high-order partitioned solver has also been extended to handle a 3-field FSI formulation. Furthermore, it has been implemented in our C++ codebase on a number of 2-field and 3-field FSI model problems and up to 5-order convergence rate has been verified.

Adjoint-based sensitivities for coupled multiphysics problems

The fully discrete sensitivity (forward) and adjoint (backward) methods corresponding to the primal solver described above have been derived. As expected, these linearized approaches inherit

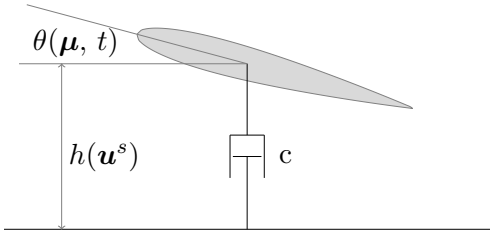

Figure 5: Airfoil in isentropic, viscous flow connected to a damper with damping constant c. The pitch of the airfoil is parametrized and the heave is determined through force balance in the vertical direction (between the force in the damper, gravity, and the force induced on the foil by the fluid).

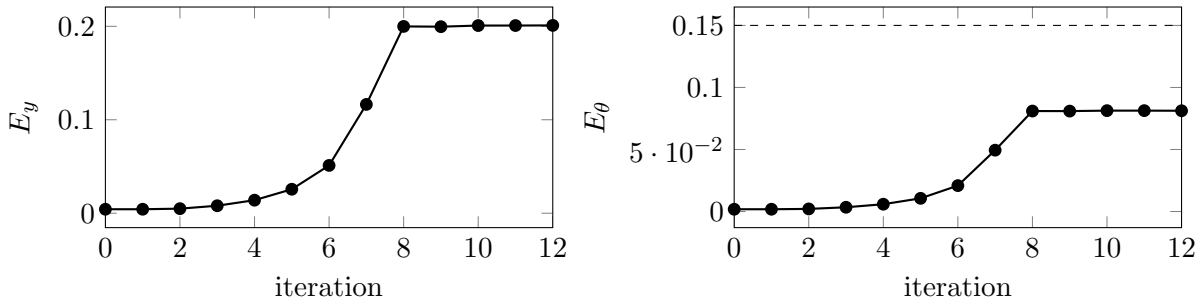

Figure 6: Convergence history of optimization solver

the partitioned nature of the primal solver and do not require specialized monolithic solvers. However, they do require matrix-vector products with derivatives (and their transpose) that do not appear in the primal solver, such as:

$$\frac{\partial \boldsymbol{r}_f}{\partial \boldsymbol{u}_s}\boldsymbol{v}, \quad \frac{\partial \boldsymbol{r}_f}{\partial \boldsymbol{u}_s}^T \boldsymbol{w}.$$

Since only matrix-vector products are required, we do not need specialized monolithic data structures that would normally be required to store $\partial \boldsymbol{r}_f / \partial \boldsymbol{u}_s$. Additionally, our extensive use of symbolic differentiation and code generation makes such terms readily available.

The fully discrete sensitivity and adjoint methods have been implemented in our C++ codebase for both the 2-field and 3-field FSI solvers and the resulting gradients of various quantities of interest have been verified with finite differences.

Results

We demonstrate the fluid-structure optimization capabilities of our code by considering the design of a fluid-mass-damper system (Figure 5) as an optimal energy harvesting mechanism. Let E_y be the energy stored in the damper, E_θ be the energy required to drive the flapping motion, and consider the optimization problem of maximizing E_y (the energy extracted from the system) subject to a bound on E_θ (a fixed budget of input energy)

$$\begin{aligned} \underset{\boldsymbol{\mu}}{\text{minimize}} \quad & E_y(\boldsymbol{\mu}) \\ \text{subject to} \quad & E_\theta(\boldsymbol{\mu}) \leq \bar{E}_\theta. \end{aligned}$$

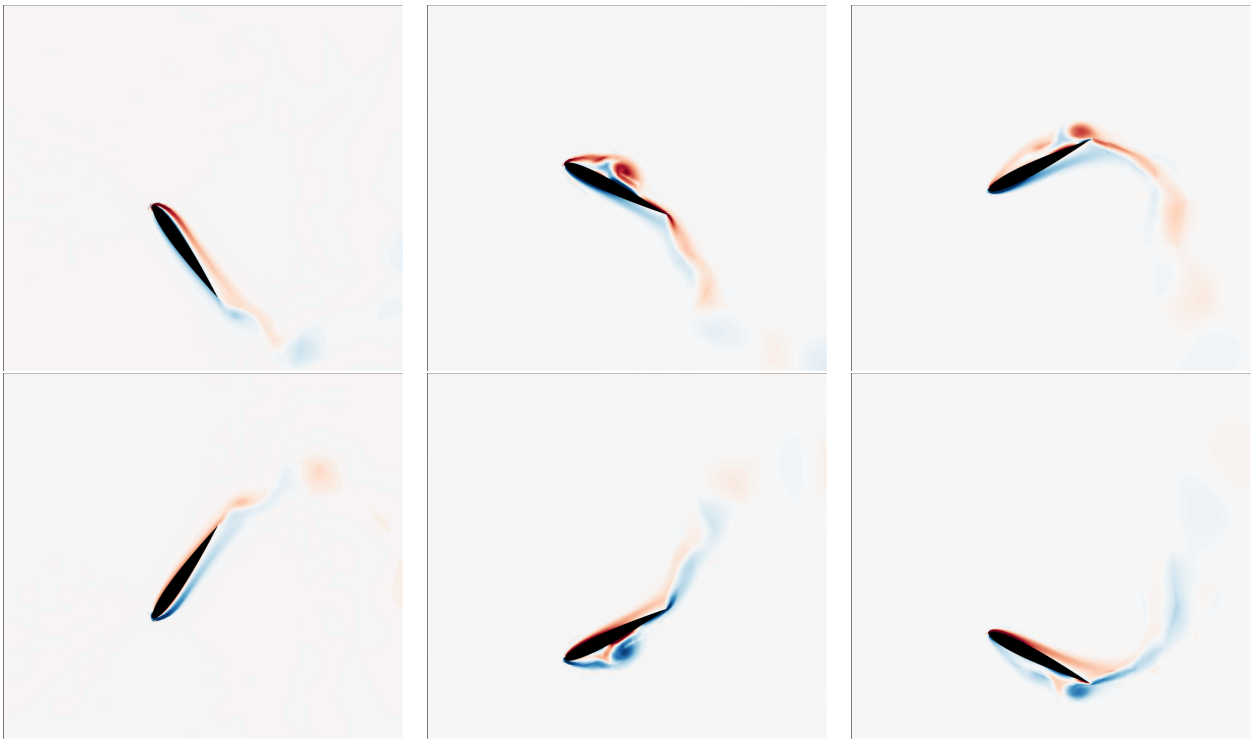

Figure 7: Flow vorticity around airfoil undergoing optimal pitching motion for energy extraction. Snapshots are taken at six equally spaced time instances.

In this problem, the parameters $\boldsymbol{\mu}$ control the trajectory of the pitching motion of the airfoil (Figure 5) and the vertical motion is determine through a force balance (a single degree of freedom structure in this preliminary FSI example). The convergence history of the optimization solver (IPOPT in this case) is shown in Figure 6; the non-smooth cutoff occurs when an optimization variable hits a bound. Within 13 iterations, the extracted energy (E_y) has increased substantially, while staying within the input energy budget. The trajectory of the airfoil and flow vorticity corresponding to the optimal pitching motion $\theta(\boldsymbol{\mu}^*, t)$ are shown in Figure 7.

Optimization-based high-order shock tracking

Here, we give a short summary of our recent work on high-order accurate curved shock tracking schemes for the discontinuous Galerkin method. For more details, see our JCP paper [26] and AIAA SciTech papers [30, 24].

Motivation

While much progress have been made in the development of high-order methods, they are still suffering from the lack of nonlinear stability. This limits their impact on many important applications, in particular ones involving shocks since even small oscillations in the solution can cause non-physical results. We have developed an alternative approach for handling shocks in a high-order DG method, which is more closely related to shock tracking and r-refinement than shock capturing. It is based on the observations that if a (curved) face of an element is perfectly aligned with a shock, the approximate Riemann solver will provide the appropriate stabilization and allow for high-order approximations of the solution on both sides of the discontinuity. The difficulty with

these methods is that the DG method without additional stabilization is highly sensitive to the location of the elements, and a very small mismatch will in general result in oscillations and prevent convergence. Instead we recast the nonlinear, discrete equations as a PDE-constrained optimization problem where the objective function is an appropriate shock indicator, the constraints are the DG discretization of the conservation law, and the optimization variables are the discrete PDE solution and the positions of the nodes of the mesh. The mesh deformation is handled by transforming the conservation law to a fixed reference domain through a diffeomorphism. This means the mesh nodes will be aligned in a consistent way with the current numerical solution (and not, e.g., the true physical position), but also that we can obtain converged solutions using efficient constrained optimization methods.

Discontinuity tracking and mesh regularization

Our shock tracking framework is based on a PDE-constrained optimization formulation:

$$\begin{aligned} \underset{\boldsymbol{u},\,\boldsymbol{\phi}}{\text{minimize}} \quad & f_{shk}(\boldsymbol{u},\,\boldsymbol{x}(\boldsymbol{\phi})) \\ \text{subject to} \quad & f^K_{msh}(\boldsymbol{x}(\boldsymbol{\phi})) \leq \bar{f}_{msh}, \quad K \in \mathcal{E}_{h,p} \\ & \boldsymbol{r}(\boldsymbol{u},\,\boldsymbol{x}(\boldsymbol{\phi})) = 0, \end{aligned} \tag{18}$$

where $f_{shk}(\boldsymbol{u},\,\boldsymbol{x})$ is a shock-indicating objective function and $f^K_{msh}(\boldsymbol{x})$ is the distortion of element $K \in \mathcal{E}_{h,p}$. This optimization problem seeks to find the mesh $\boldsymbol{x}(\boldsymbol{\phi})$ and solution $\boldsymbol{u}$ that minimize $f_{shk}(\boldsymbol{u},\,\boldsymbol{x})$ while satisfying the discretized PDE and mesh quality constraints.

The indicator used in this work is the integrated deviation of the solution from the mean in each element:

$$f_{shk}(\boldsymbol{u},\,\boldsymbol{x}) = \sum_{K \in \mathcal{E}_{h,p}} \int_{\mathcal{G}(K,\,\boldsymbol{x})} \left\| u_{h,p} - \bar{u}^K_{h,p} \right\|^2_{\boldsymbol{W}} \, dV \tag{19}$$

where the dependence of the finite dimensional solution $u_{h,p}$ on the discrete representation is implied, $\bar{u}^K_{h,p}$ is the mean value of $u_{h,p}$ over element K, and $\boldsymbol{W} \in \mathbb{R}^{N_c \times N_c}$ is the symmetric positive semi-definite matrix that defines the local semi-norm,

$$\bar{u}^K_{h,p} = \frac{1}{|\mathcal{G}(K,\,\boldsymbol{x})|} \int_{\mathcal{G}(K,\,\boldsymbol{x})} u_{h,p} \, dV, \qquad |\mathcal{G}(K,\,\boldsymbol{x})| = \int_{\mathcal{G}(K,\,\boldsymbol{x})} dV. \tag{20}$$

The discontinuity indicator in (19) is not well-suited as the objective function in the discontinuity-tracking optimization setting (18) in its current form because it is agnostic to a poor quality or inverted mesh that may arise from certain choices of $\boldsymbol{x}$. To avoid the mesh distortion that would result from solely minimizing f_{shk}, we include constraints on the elementwise mesh distortion in (18). Here, we define the mesh distortion as the deviation from the uniform element in one dimension and utilize a common mesh distortion metric in high-order mesh generation in higher dimensions

$$f^K_{msh}(\boldsymbol{x}) = \begin{cases} \left| \dfrac{h_0}{|\mathcal{G}(K,\,\boldsymbol{x})|} - 1 \right| & d = 1 \\ \dfrac{1}{|\mathcal{G}(K,\,\boldsymbol{x})|} \displaystyle\int_{\mathcal{G}(K,\,\boldsymbol{x})} \left(\frac{\|G_{h,p}\|^2_F}{(\det G_{h,p})^{2/d}_+} \right)^r & \text{otherwise,} \end{cases} \tag{21}$$

for $K \in \mathcal{E}_{h,p}$, where $r = 2$ is used in this work and $G_{h,p} = \dfrac{\partial x_{h,p}}{\partial X}$ is the finite-dimensional deformation gradient.

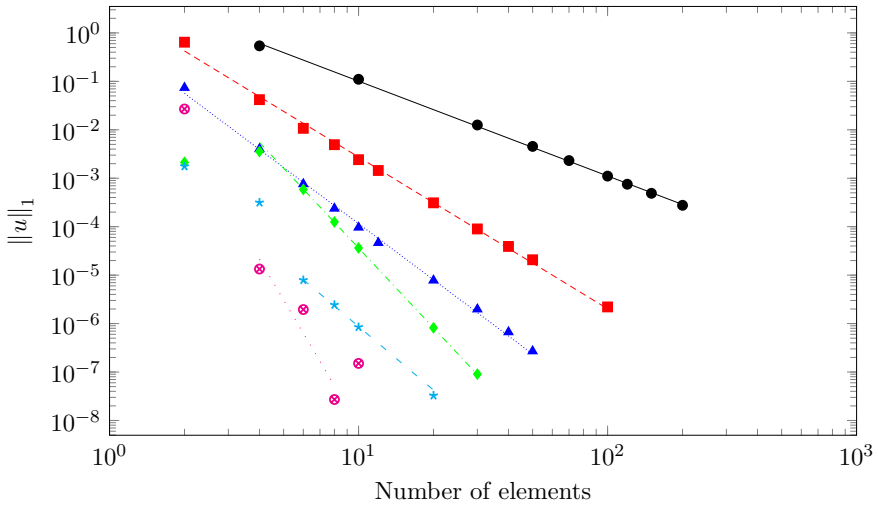

Figure 8: Burgers' equation with shock tracking: $p = 1$ (●), $p = 2$ (■), $p = 3$ (▲), $p = 4$ (♦), $p = 5$ (⋆), $p = 6$ (⊗). Slopes: $\angle -1.95$ (——), $\angle -3.13$ (- - - -), $\angle -3.85$ (·····), $\angle -5.47$ (- · - · -), $\angle -4.36$ (- -), $\angle -8.67$ (· · ·).

The optimization problem in (18) is solved using a full space approach that treats $\boldsymbol{u}$ and $\boldsymbol{\phi}$ as independent optimization variables and converges them simultaneously to their optimal values. This implies the solution of the PDE is *never required away from a discontinuity-aligned mesh* $\boldsymbol{x}^*$ and overcomes potential stability issues that would arise in a reduced space approach that requires the solution of the PDE at unconverged (and therefore non-aligned) meshes.

Results

In Figure 8, we should a convergence study for a model steady-state Burgers' equation problem with a fully developed shock. The shock location is unknown to the solver, but found using our full space solution approach and we obtain high-order convergence with remarkable accuracy for as few as 10 elements.

A two-dimensional example is shown in Figure 9. The 2D Euler equations are solved for supersonic flow around a cylinder at Mach 2. Already at polynomial degrees $p = 2$ the shock is well-resolved by the curved elements, and again remarkable accuracy is obtained with as few as 48 high-order elements. Note that typical low-order schemes would require 10,000s of anisotropic elements to accurately resolve this shock.

Shock boundary-layer interaction with LES

We have applied many of our techniques to a highly challenging and important problem in CFD – the transonic buffet on an airfoil at Reynolds number 3 million. The results are presented in [28], here we summarize the findings.

Motivation

Transonic flow over an airfoil can result in complex interactions between shock waves and the viscous boundary layer. A particularly interesting and challenging phenomenon is that of transonic buffet, whereby the flow separation induces instabilities, unsteady behavior and structural

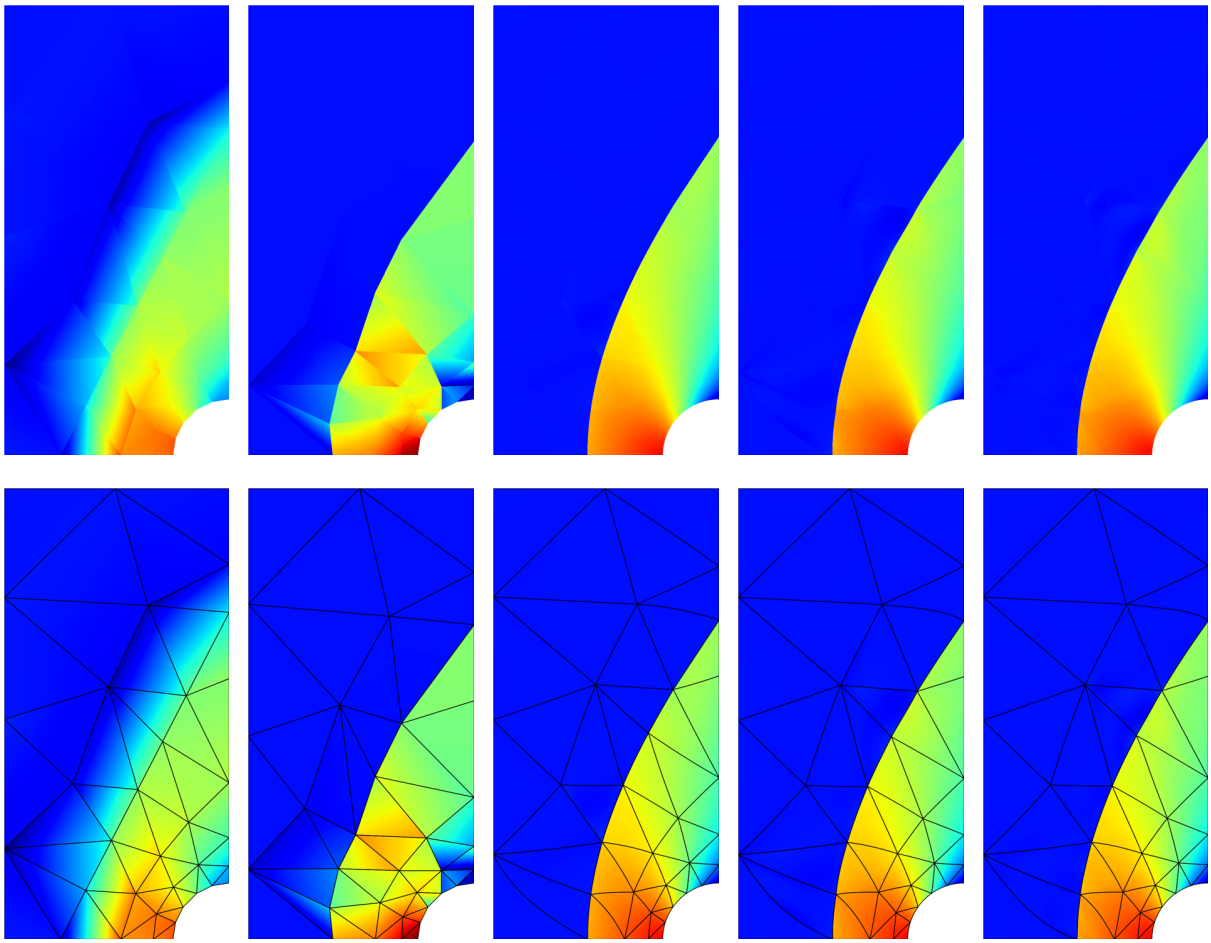

Figure 9: Resolution of 2D supersonic flow with only 48 elements. **Density** (ρ): *Far left* – initial guess, solved with artificial viscosity and non-aligned mesh. *Remaining*: Solutions with shock tracking framework, using 48 elements of degree $p = 1, 2, 3, 4$.

vibrations, termed buffeting. This strong phenomenon can cause dangerous vibrations leading to the destruction of a wing or a turbomachine blade. The origin and onset of transonic buffet has been studied experimentally, in the context of global stability theory, and computationally, using a variety of discretizations and approaches.

The numerical simulation of transonic buffet on airfoils is highly challenging, due to its unsteady nature, the turbulent flows, and the complex interaction between shocks and flow separation. Most of the standard tools in computational fluid dynamics for modeling turbulence are based on the unsteady Reynolds-averaged Navier-Stokes (URANS) equations, which are widely believed to produce unreliable results for massively separated unsteady flows. Alternative approaches such as large eddy simulation (LES) and hybrid methods such as detached eddy simulation (DES) are typically better at modeling these flow problems, however at several magnitudes higher computational cost.

In this work, we apply a state-of-the-art high-order DG solver to the simulation of transonic buffet on the ONERA OAT15A airfoil. This is a well-studied model problem with many experimental and numerical results to compare with. Our main focus is to evaluate our high-order methods for modeling this phenomenon, in particular with respect to (a) the numerical stability of the solvers and the high-order approximations, and (b) the accuracy of the resulting flow predictions. A fundamental difficulty with high-order methods is the treatment and stabilization of shocks and other under-resolved features of the solution. Here, we use the artificial visocisty approach developed previously in our group, which achieves subgrid resolution using a highly sensitive indicator based on orthogonal polynomials.

Results

We show here some of the preliminary results of our simulations. Figure 10 shows the averaged pressure coefficients for a range of meshes and simulation cases, together with the RMS fluctuations. We note that this problem is highly challenging, and the DES simulations by Huang et al are considered in fairly good agreement with experiments. Our results are similarly accurate, however the 2D results have a secondary shock structure that is likely a non-physical phenomenon. In 3D the results are good but likely need longer simulation times for more accurate averaging, which is our plans for future work.

Snapshots of the 3D solution are shown in figure 11, clearly showing the oscillating shock as well as the complex turbulent flow structures.

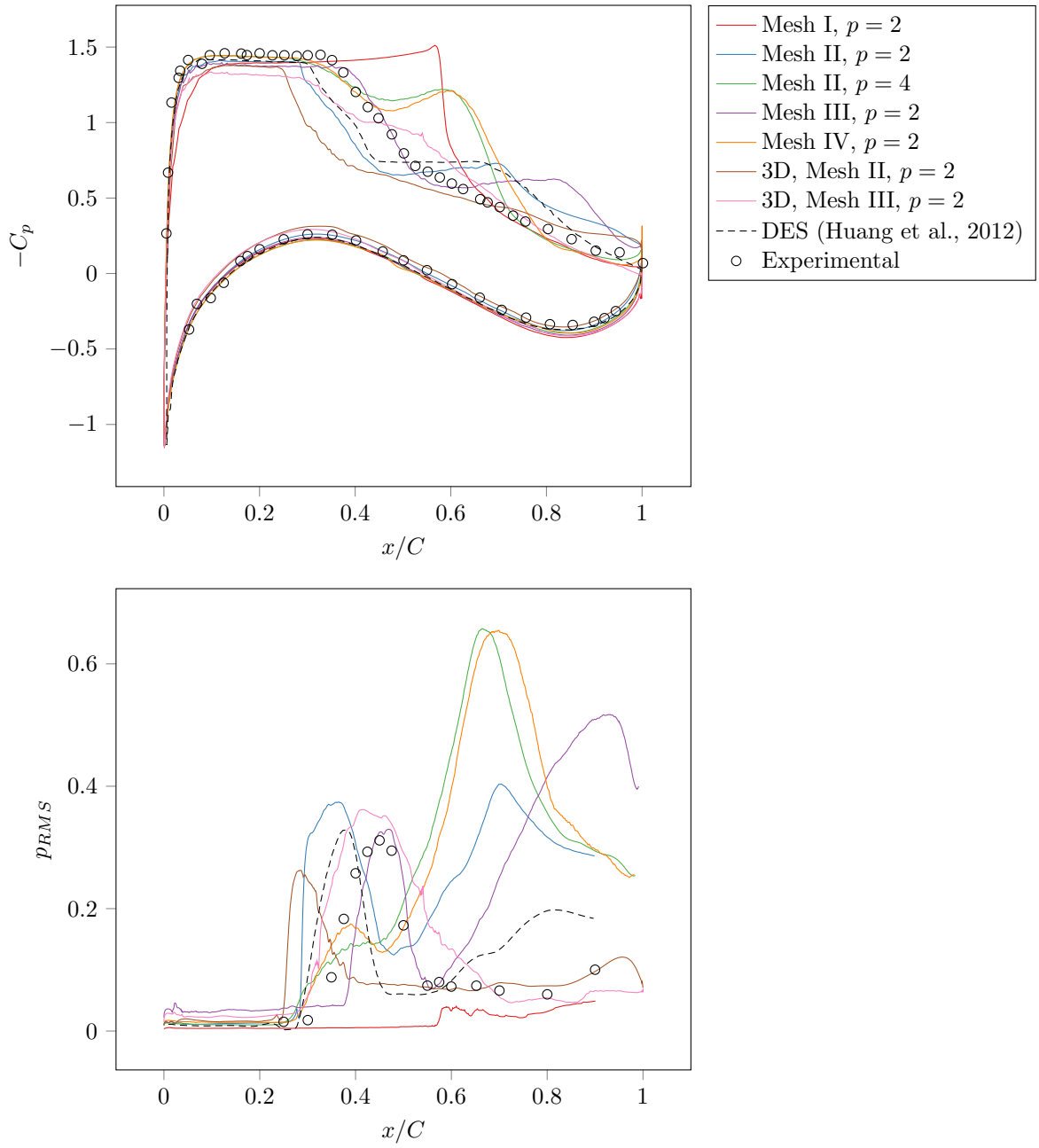

Figure 10: Left: coefficient of pressure for the OAT15A airfoil using various simulation configurations. Right: RMS pressure fluctuations on the suction side of the airfoil for the same configurations.

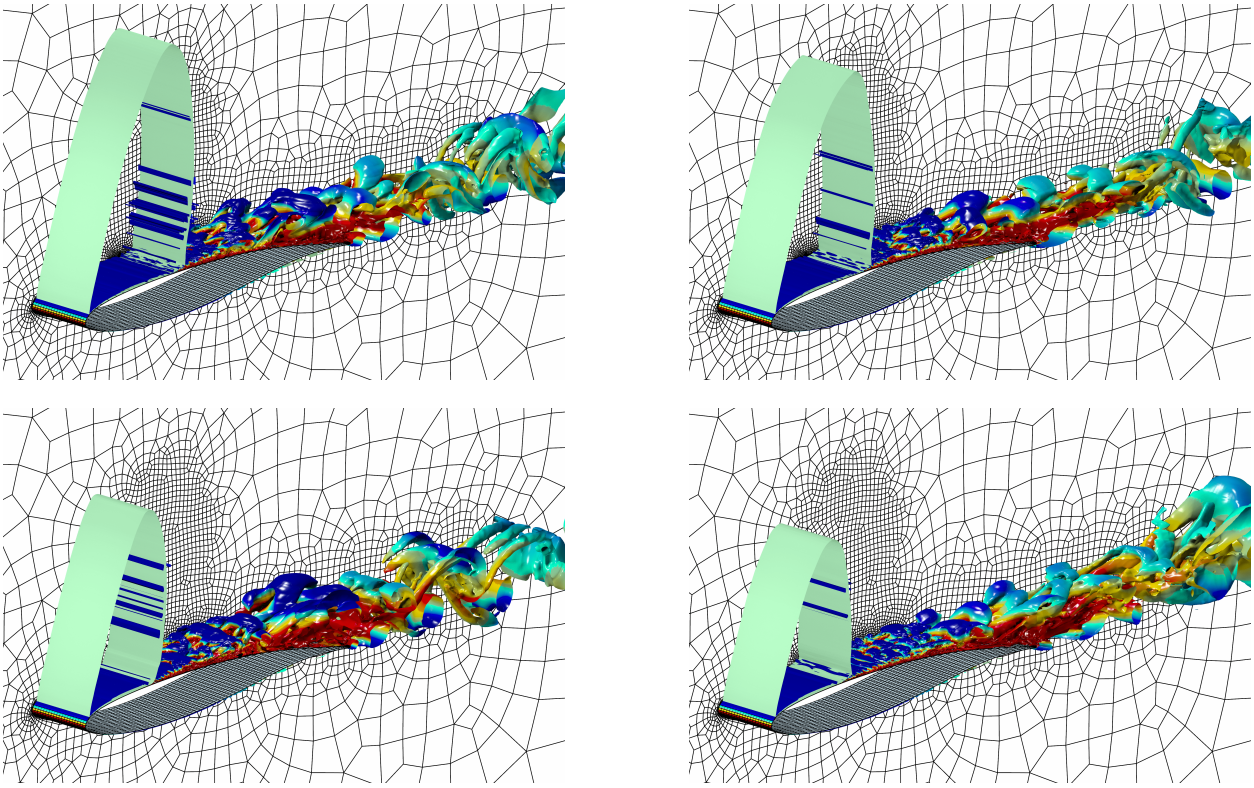

Figure 11: Snapshots of 3D solution, showing isosurfaces of Q-criterion, colored by velocity magnitude. The location of the shock is visualized in green using a Mach 1 isosurface.

Personnel Supported

- Per-Olof Persson, Principal Investigator, Dept. of Mathematics, UC Berkeley
- Michael Franco, Ph.D. student, Dept. of Mathematics, UC Berkeley
- Meire Fortunato, Ph.D. student, Dept. of Mathematics, UC Berkeley
- Danny Hermes, Ph.D. student, Dept. of Mathematics, UC Berkeley
- Noble Macfarlane, Ph.D. student, Dept. of Mathematics, UC Berkeley
- Will Pazner, Ph.D. student, Dept. of Mathematics, UC Berkeley
- Andrew Shi, Ph.D. student, Dept. of Mathematics, UC Berkeley
- Jingyi Wang, Ph.D. student, Dept. of Mech. Engr., UC Berkeley
- Luming Wang, Ph.D. student, Dept. of Mathematics, UC Berkeley

Transitions/Interactions

Conference Professional Activities

- Committee member, 5th International Workshop on High-Order CFD Methods, January 2018
- Committee member, 25th International Meshing Roundtable, October 2016
- Mini-symposium organizer, 12th World Congress on Computational Mechanics, July 2016
- Committee member, 4th International Workshop on High-Order CFD Methods, June 2016
- Committee member, 24th International Meshing Roundtable, October 2015
- Mini-symposium organizer, U.S. National Congress on Computational Mechanics, July 2015
- Committee member, 3rd International Workshop on High-Order CFD Methods, January 2015

Conference, Colloquia and Workshop Presentations

- AIAA Scitech 2019, San Diego, CA, January 2019
- Texam A&M University, Numerical Analysis Seminar, College Station, TX, Nov 2018
- UC Santa Barbara, Mechnical Engineering Colloquium, Santa Barbara, CA, Oct 2018
- AFOSR Computational Mathematics Program Review, Arlington, VA, August 2018
- Stanford University, CompGeo seminar, Palo Alto, CA, February 2018
- AIAA Scitech 2018, Orlando, FL, January 2018
- AFOSR Computational Mathematics Program Review, Arlington, VA, August 2017
- AIAA Aviation, Denver, CO, June 2017
- FEF 2017, Rome, Italy, April 2017
- HONOM 2017, Stuttgart, Germany, March 2017
- SIAM Conference on Computational Science and Engineering, Atlanta, GA, February 2017
- RWTH Aachen, MathCCES seminar, Aachen, Germany, December 2017
- Lund University, Centre for Mathematical Sciences, Lund, Sweden, November 2017
- AFOSR Computational Mathematics Program Review, Arlington, VA, August 2016
- 12th World Congress on Computational Mechanics (WCCM 2016), Seoul, Korea, July 2016
- NIMS Workshop on Higher order methods, Daejeon, Korea, July 2016
- ECCOMAS Congress 2016, Crete Island, Greece, June 2016
- University of Chicago, Scientific and Statistical Computing Seminar, Chicago, IL, May 2016
- Université Pierre et Marie Curie (Paris VI), Séminaire du LJLL, Paris, France, Nov. 2015
- Department of EECS, UC Berkeley, Berkeley, CA, September 2015

- Mathematisches Forschungsinstitut workshop, Oberwolfach, Germany, September 2015
- AFOSR Computational Mathematics Program Review, Arlington, VA, August 2015
- 13th U.S. National Congress on Computational Mechanics, San Diego, CA, July 2015
- 22nd AIAA Computational Fluid Dynamics Conference, Dallas, TX, June 2015
- UT Austin, ICES Seminar, Austin, TX, April 2015
- SIAM Computational Science and Engineering, Salt Lake City, UT, March 2015
- Antony Jameson's 80th Birthday Conference, Stanford University, November 2014

Open-Source Software

- Bézier: Helper for Bézier Curves, Triangles, and Higher Order Objects, at `https://github.com/dhermes/bezier`

New Discoveries, Inventions, or Patent Disclosures

None

Honors/Awards

- W. Pazner: First place in the Student Paper Competition in CFD, 23rd AIAA Computational Fluid Dynamics Conference, in Denver, CO, June 2017
- M. Fortunato: Best Poster Award, 24th International Meshing Roundtable, October 2015

Acknowledgment/Disclaimer

This work was sponsored (in part) by the Air Force Office of Scientific Research, USAF, under grant/contract number FA9550-15-1-0010. The views and conclusions contained herein are those of the authors and should not be interpreted as necessarily representing the official policies or endorsements, either expressed or implied, of the Air Force Office of Scientific Research or the U.S. Government.

Publications

[1] B. Froehle and P.-O. Persson. A high-order discontinuous Galerkin method for fluid-structure interaction with efficient implicit-explicit time stepping. *J. Comput. Phys.*, 272:455–470, 2014.

[2] L. Wang and P.-O. Persson. High-order discontinuous Galerkin simulations on moving domains using an ale formulation and local remeshing with projections. In *53rd AIAA Aerospace Sciences Meeting, Orlando, Florida*, 2015. AIAA-2015-0820.

[3] L. Wang. *Discontinuous Galerkin Methods on Moving Domains with Large Deformations*. PhD thesis, University of California, Berkeley, 2015.

[4] L. Wang and P.-O. Persson. A high-order discontinuous Galerkin method with unstructured space-time meshes for two-dimensional compressible flows on domains with large deformations. *Comput. & Fluids*, 118:53–68, 2015.

[5] S. Kanner and P.-O. Persson. Magnitude and frequency of forces on a low-Reynolds VAWT airfoil using high-order LES. In *AIAA SciTech 33rd Wind Energy Symposium, Orlando, FL*, 2015. AIAA-2015-0218.

[6] L. Wang and P.-O. Persson. A high-order discontinuous Galerkin method with unstructured space–time meshes for two-dimensional compressible flows on domains with large deformations. *Comput. & Fluids*, 118:53–68, 2015.

[7] L. Wang and P.-O. Persson. High-order discontinuous Galerkin simulations on moving domains using an ALE formulation and local remeshing with projections. In *53rd AIAA Aerospace Sciences Meeting, Orlando, FL*, 2015. AIAA-2015-0820.

[8] B. Froehle and P.-O. Persson. Nonlinear elasticity for mesh deformation with high-order discontinuous Galerkin methods for the Navier-Stokes equations on deforming domains. In *Spectral and High Order Methods for Partial Differential Equations ICOSAHOM 2014*, volume 106, pages 73–85, 2015.

[9] M. J. Zahr, P.-O. Persson, and J. Wilkening. A fully discrete adjoint method for optimization of flow problems on deforming domains with time-periodicity constraints. *Comput. & Fluids*, 139:130–147, 2016.

[10] M. J. Zahr and P.-O. Persson. An adjoint method for a high-order discretization of deforming domain conservation laws for optimization of flow problems. *J. Comput. Phys.*, 326:516–543, 2016.

[11] S. Kanner and P.-O. Persson. Validation of a high-order large-eddy simulation solver using a vertical- axis wind turbine. *AIAA journal*, 54(1):101–112, 2016.

[12] S. Kanner and P.-O. Persson. Implicit large-eddy simulations of 2D counter-rotating vertical-axis wind turbines. In *AIAA SciTech 34th Wind Energy Symposium, San Diego, CA*, 2016. AIAA-2016-1731.

[13] M. Fortunato and P.-O. Persson. High-order unstructured curved mesh generation using the Winslow equations. *J. Comput. Phys.*, 307:1–14, 2016.

[14] M. Zahr and P.-O. Persson. High-order, time-dependent aerodynamic optimization using a discontinuous Galerkin discretization of the navier-stokes equations. In *2016 AIAA Aerospace Sciences Meeting, San Diego, CA*, 2016.

[15] S. Kanner, L. Wang, and P.-O. Persson. Implicit large-eddy simulations of 2d counter-rotating vertical-axis wind turbines. In *2016 AIAA SciTech 34th Wind Energy Symposium, San Diego, CA*, 2016.

[16] W. Pazner and P.-O. Persson. Stage-parallel fully implicit Runge-Kutta solvers for discontinuous Galerkin fluid simulations. *J. Comput. Phys.*, 335:700–717, 2017.

[17] W. Pazner and P.-O. Persson. High-order DNS and LES simulations using an implicit tensor-product discontinuous Galerkin method. In *23rd AIAA Computational Fluid Dynamics Conference, Denver, CO*, 2017. AIAA-2017-3948.

[18] J. Wang, M. Zahr, and P.-O. Persson. Energetically optimal flapping flight via a fully discrete adjoint method with explicit treatment of flapping frequency. In *23rd AIAA Computational Fluid Dynamics Conference, Denver, CO*, 2017. AIAA-2017-4412.

[19] M. J. Zahr and P.-O. Persson. Energetically optimal flapping wing motions via adjoint-based optimization and high-order discretizations. In *Frontiers in PDE Constrained Optimization*. Springer, 2017.

[20] W. Pazner and P.-O. Persson. On the convergence of iterative solvers for polygonal discontinuous Galerkin discretizations. *Commun. Appl. Math. Comput. Sci.*, 13(1):27–51, 2018.

[21] W. Pazner and P.-O. Persson. Approximate tensor-product preconditioners for very high order discontinuous Galerkin methods. *J. Comput. Phys.*, 354:344–369, 2018.

[22] W. Pazner and P.-O. Persson. Very high-order symmetric interior penalty discontinuous Galerkin methods for LES flows using implicit tensor-product solvers. In *2018 AIAA Aerospace Sciences Meeting, Kissimmee, FL*, 2018.

[23] M. J. Zahr and P.-O. Persson. Adjoint-based optimization of time-dependent fluid-structure systems using a high-order discontinuous Galerkin discretization. In *2018 AIAA Aerospace Sciences Meeting, Kissimmee, FL*, 2018.

[24] M. J. Zahr and P.-O. Persson. An optimization based discontinuous Galerkin approach for high-order accurate shock tracking. In *2018 AIAA Aerospace Sciences Meeting, Kissimmee, FL*, 2018.

[25] S. Kanner and P.-O. Persson. High-order wall-modeled large-eddy simulation of counter-rotating vertical-axis wind turbines. In *2018 Wind Energy Symposium, AIAA Science and Technology Forum and Exposition 2018, Kissimmee, FL*, 2018.

[26] M. J. Zahr and P.-O. Persson. An optimization-based approach for high-order accurate discretization of conservation laws with discontinuous solutions. *J. Comput. Phys.*, 365:105–134, 2018.

[27] D. Z. Huang, P.-O. Persson, and M. Zahr. A high-order partitioned solver for general multiphysics problems and its applications in optimization. In *2019 AIAA Aerospace Sciences Meeting, San Diego, CA*, 2019.

[28] W. Pazner, M. Franco, and P.-O. Persson. High-order wall-resolved large eddy simulation of transonic buffet on the OAT15A airfoil. In *2019 AIAA Aerospace Sciences Meeting, San Diego, CA*, 2019.

[29] M. Franco, P.-O. Persson, W. Pazner, and M. Zahr. An adjoint method using fully implicit Runge-Kutta schemes for optimization of flow problems. In *2019 AIAA Aerospace Sciences Meeting, San Diego, CA*, 2019.

[30] A. Shi, P.-O. Persson, and M. Zahr. An optimization-based discontinuous Galerkin approach for high-order accurate shock tracking with guaranteed mesh quality. In *2019 AIAA Aerospace Sciences Meeting, San Diego, CA*, 2019.

[31] D. Z. Huang, P.-O. Persson, and M. J. Zahr. High-order, linearly stable, partitioned solvers for general multiphysics problems based on implicit–explicit Runge–Kutta schemes. *Computer Methods in Applied Mechanics and Engineering*, 346:674–706, 2019.

AFOSR Deliverables Submission Survey

Response ID:10893 Data

1.

Report Type

Final Report

Primary Contact Email

Contact email if there is a problem with the report.

persson@berkeley.edu

Primary Contact Phone Number

Contact phone number if there is a problem with the report

510-520-5245

Organization / Institution name

University of California, Berkeley

Grant/Contract Title

The full title of the funded effort.

Efficient and Robust High-Order Methods for Fluid and Solid Mechanics

Grant/Contract Number

AFOSR assigned control number. It must begin with "FA9550" or "F49620" or "FA2386".

FA9550-15-1-0010

Principal Investigator Name

The full name of the principal investigator on the grant or contract.

Per-Olof Persson

Program Officer

The AFOSR Program Officer currently assigned to the award

Dr. Fariba Fahroo

Reporting Period Start Date

11/01/2014

Reporting Period End Date

10/31/2018

Abstract

The goal of the project was to develop new numerical schemes and solvers for high-order accurate simulations of problems in fluid and solid mechanics. Three main areas were addressed -- space-time methods for domains with large deformations, implicit matrix-free solvers for sparse line-based discretizations, and applications to problems with highly turbulent flow. The project has led to significant developments in space-time mesh generation for complex flow problems, entropy stable line-based discontinuous Galerkin discretizations, low-memory Kronecker SVD factorizations applied to preconditioning, practical solvers for fully implicit Runge-Kutta methods, partitioned multiphysics solvers based on IMEX schemes, and new high-order schemes for shock tracking. The results were applied to important real-world
problems, such as the high-order simulation of shock boundary-layer interaction. The findings were disseminated through a

wide range of publications, presentations, and public domain software.

Distribution Statement

This is block 12 on the SF298 form.

Distribution A - Approved for Public Release

Explanation for Distribution Statement

If this is not approved for public release, please provide a short explanation. E.g., contains proprietary information.

SF298 Form

Please attach your SF298 form. A blank SF298 can be found here. Please do not password protect or secure the PDF The maximum file size for an SF298 is 50MB.

persson_sr298.pdf

Upload the Report Document. File must be a PDF. Please do not password protect or secure the PDF . The maximum file size for the Report Document is 50MB.

persson_final.pdf

Upload a Report Document, if any. The maximum file size for the Report Document is 50MB.

Archival Publications (published) during reporting period:

[1] B. Froehle and P.-O. Persson. A high-order discontinuous Galerkin method for fluid-structure interaction with efficient implicit-explicit time stepping. J. Comput. Phys., 272:455–470, 2014.

[2] L. Wang and P.-O. Persson. High-order discontinuous Galerkin simulations on moving domains using an ale formulation and local remeshing with projections. In 53rd AIAA Aerospace Sciences Meeting, Orlando, Florida, 2015. AIAA-2015-0820.

[3] L. Wang. Discontinuous Galerkin Methods on Moving Domains with Large Deformations. PhD thesis, University of California, Berkeley, 2015.

[4] L. Wang and P.-O. Persson. A high-order discontinuous Galerkin method with unstructured space-time meshes for two-dimensional compressible flows on domains with large deformations. Comput. & Fluids, 118:53–68, 2015.

[5] S. Kanner and P.-O. Persson. Magnitude and frequency of forces on a low-Reynolds VAWT airfoil using high-order LES. In AIAA SciTech 33rd Wind Energy Symposium, Orlando, FL, 2015. AIAA-2015-0218.

[6] L. Wang and P.-O. Persson. A high-order discontinuous Galerkin method with unstructured space–time meshes for two-dimensional compressible flows on domains with large deformations. Comput. & Fluids, 118:53–68, 2015.

[7] L. Wang and P.-O. Persson. High-order discontinuous Galerkin simulations on moving domains using an ALE formulation and local remeshing with projections. In 53rd AIAA Aerospace Sciences Meeting, Orlando, FL, 2015. AIAA-2015-0820.

[8] B. Froehle and P.-O. Persson. Nonlinear elasticity for mesh deformation with high-order discontinuous Galerkin methods for the Navier-Stokes equations on deforming domains. In Spectral and High Order Methods for Partial Differential Equations ICOSAHOM 2014, volume 106, pages 73–85, 2015.

[9] M. J. Zahr, P.-O. Persson, and J. Wilkening. A fully discrete adjoint method for optimization of flow problems on deforming domains with time-periodicity constraints. Comput. & Fluids, 139:130–147, 2016.

[10] M. J. Zahr and P.-O. Persson. An adjoint method for a high-order discretization of deforming domain conservation laws for optimization of flow problems. J. Comput. Phys., 326:516–543, 2016.

[11] S. Kanner and P.-O. Persson. Validation of a high-order large-eddy simulation solver using a vertical-axis wind turbine. AIAA journal, 54(1):101–112, 2016.

[12] S. Kanner and P.-O. Persson. Implicit large-eddy simulations of 2D counter-rotating vertical-axis wind turbines. In AIAA SciTech 34th Wind Energy Symposium, San Diego, CA, 2016. AIAA-2016-1731.

[13] M. Fortunato and P.-O. Persson. High-order unstructured curved mesh generation using the Winslow equations. J. Comput. Phys., 307:1–14, 2016.

[14] M. Zahr and P.-O. Persson. High-order, time-dependent aerodynamic optimization using a discontinuous Galerkin discretization of the navier-stokes equations. In 2016 AIAA Aerospace Sciences Meeting, San Diego, CA, 2016.

[15] S. Kanner, L. Wang, and P.-O. Persson. Implicit large-eddy simulations of 2D counter-rotating vertical-axis wind turbines. In 2016 AIAA SciTech 34th Wind Energy Symposium, San Diego, CA, 2016.

[16] W. Pazner and P.-O. Persson. Stage-parallel fully implicit Runge-Kutta solvers for discontinuous Galerkin fluid simulations. J. Comput. Phys., 335:700–717, 2017.

[17] W. Pazner and P.-O. Persson. High-order DNS and LES simulations using an implicit tensor-product discontinuous Galerkin method. In 23rd AIAA Computational Fluid Dynamics Conference, Denver, CO, 2017. AIAA-2017-3948.

[18] J. Wang, M. Zahr, and P.-O. Persson. Energetically optimal flapping flight via a fully discrete adjoint method with explicit treatment of flapping frequency. In 23rd AIAA Computational Fluid Dynamics Conference, Denver, CO, 2017. AIAA-2017-4412.

[19] M. J. Zahr and P.-O. Persson. Energetically optimal flapping wing motions via adjoint-based optimization and high-order discretizations. In Frontiers in PDE Constrained Optimization. Springer, 2017.

[20] W. Pazner and P.-O. Persson. On the convergence of iterative solvers for polygonal discontinuous Galerkin discretizations. Commun. Appl. Math. Comput. Sci., 13(1):27–51, 2018.

[21] W. Pazner and P.-O. Persson. Approximate tensor-product preconditioners for very high order discontinuous Galerkin methods. J. Comput. Phys., 354:344–369, 2018.

[22] W. Pazner and P.-O. Persson. Very high-order symmetric interior penalty discontinuous Galerkin methods for LES flows using implicit tensor-product solvers. In 2018 AIAA Aerospace Sciences Meeting, Kissimmee, FL, 2018.

[23] M. J. Zahr and P.-O. Persson. Adjoint-based optimization of time-dependent fluid-structure systems using a high-order discontinuous Galerkin discretization. In 2018 AIAA Aerospace Sciences Meeting, Kissimmee, FL, 2018.

[24] M. J. Zahr and P.-O. Persson. An optimization based discontinuous Galerkin approach for high-order accurate shock tracking. In 2018 AIAA Aerospace Sciences Meeting, Kissimmee, FL, 2018.

[25] S. Kanner and P.-O. Persson. High-order wall-modeled large-eddy simulation of counter-rotating vertical-axis wind turbines. In 2018 Wind Energy Symposium, AIAA Science and Technology Forum and Exposition 2018, Kissimmee, FL, 2018.

[26] M. J. Zahr and P.-O. Persson. An optimization-based approach for high-order accurate discretization of conservation laws with discontinuous solutions. J. Comput. Phys., 365:105–134, 2018.

[27] D. Z. Huang, P.-O. Persson, and M. Zahr. A high-order partitioned solver for general multiphysics problems and its applications in optimization. In 2019 AIAA Aerospace Sciences Meeting, San Diego, CA, 2019.

[28] W. Pazner, M. Franco, and P.-O. Persson. High-order wall-resolved large eddy simulation of transonic buffet on the

OAT15A airfoil. In 2019 AIAA Aerospace Sciences Meeting, San Diego, CA, 2019.

[29] M. Franco, P.-O. Persson, W. Pazner, and M. Zahr. An adjoint method using fully implicit Runge-Kutta schemes for optimization of flow problems. In 2019 AIAA Aerospace Sciences Meeting, San Diego, CA, 2019.

[30] A. Shi, P.-O. Persson, and M. Zahr. An optimization-based discontinuous Galerkin approach for high-order accurate shock tracking with guaranteed mesh quality. In 2019 AIAA Aerospace Sciences Meeting, San Diego, CA, 2019.

[31] D. Z. Huang, P.-O. Persson, and M. J. Zahr. High-order, linearly stable, partitioned solvers for general multiphysics problems based on implicit–explicit Runge–Kutta schemes. Computer Methods in Applied Mechanics and Engineering, 346:674–706, 2019.

New discoveries, inventions, or patent disclosures:

Do you have any discoveries, inventions, or patent disclosures to report for this period?

No

Please describe and include any notable dates

Do you plan to pursue a claim for personal or organizational intellectual property?

Changes in research objectives (if any):

None

Change in AFOSR Program Officer, if any:

Dr. Jean-Luc Cambier was Program Officer for a few years during the award period.

Extensions granted or milestones slipped, if any:

None

AFOSR LRIR Number

LRIR Title

Reporting Period

Laboratory Task Manager

Program Officer

Research Objectives

Technical Summary

Funding Summary by Cost Category (by FY, $K)

	Starting FY	FY+1	FY+2
Salary			
Equipment/Facilities			
Supplies			
Total			

Report Document

Report Document - Text Analysis

Report Document - Text Analysis

Appendix Documents

2. Thank You

E-mail user

Jan 31, 2019 22:06:44 Success: Email Sent to: persson@berkeley.edu